Powder Technology

Volume 292, May 2016, Pages 342–350

An assessment of triboelectrification effects on co-ground solid dispersions of carbamazepine

Adeola O Adebisi[a], Waseem Kaialy[b], Tariq Hussain[c], Hiba Al-Hamidi[d], Ali Nokhodchi[e], Barbara R. Conway[a], Kofi Asare-Addo[a]*

[a]Department of Pharmacy, University of Huddersfield, Huddersfield, HD1 3DH, UK

[b]School of Pharmacy, University of Wolverhampton, Faculty of Science and Engineering, Wolverhampton, WV1 1LY, UK

[c]The Wolfson Centre for Bulk Solids Handling Technology, Medway School of Engineering, University of Greenwich, Kent, UK

[d]Medway School of Pharmacy, Universities of Kent, Central Avenue, Kent, ME4 4TB, UK

[e]School of Life Sciences, University of Sussex, JMS Building, Falmer, Brighton, UK

*Corresponding author (Kofi Asare-Addo)

e-mail: k.asare-addo@hud.ac.uk

Tel: +44 1484 472360

Fax: +44 1484 472182

Graphical abstract:

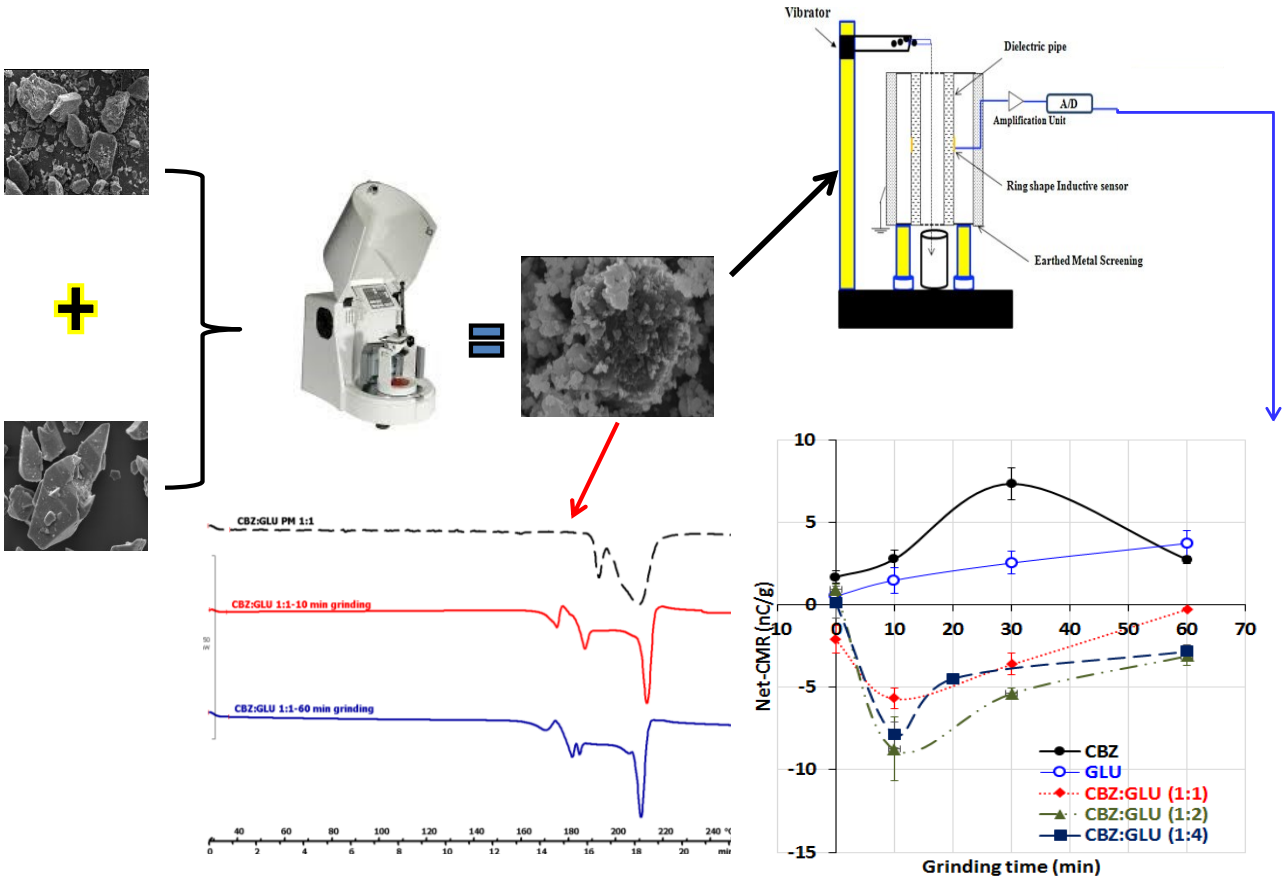

Highlights

1. The cogrinding process produced polymorphic transformations in CBZ

2. GLU exhibited lower charge densities as compared to CBZ

3. Net charge density decreases with increasing CBZ content up to 30 % above which net charge density increases

4. Technique could be used to determine appropriate formulations that improve handling

Abstract

One of strategies adopted to improve the dissolution rates of poorly soluble drugs is by co-grinding the drug with a hydrophilic carrier. However, the introduction of mechanical forces during the grinding process can lead to changes in the physicochemical characteristics as well as an increase in the surface free energy of the ground particles, which causes an alteration in the electrostatic properties of these particles. The solid state characteristics of glucosamine hydrochloride (GLU) and carbamazepine (CBZ) and their co-ground mixtures were studied using DSC, XRPD and SEM. These revealed that polymorphic transformations occurred due to the grinding process. The influence of grinding time on the triboelectrification properties of the formulations was also studied. Both pure CBZ and GLU powders were predominantly electro-positively charged and their charging properties increased with increasing grinding time. CBZ:GLU physical mixtures exhibited complicated bipolar charging behaviour, however, when subjected to grinding, these mixtures demonstrated mainly electronegative charge properties. The influence of both grinding time and CBZ content within CBZ:GLU mixtures were examined. The value of net-electronegative-charge density of CBZ:GLU mixtures was shown to increase with grinding time and /or when increasing the percentage proportion of CBZ up to 30 % w:w. This study helps to provide information about the handling of these formulation and gives a formulator tools to ascertain appropriate ratios for handling and possible simultaneous dissolution improvements.

Keywords: Electrostatics; Solid dispersions; Triboelectrification; Carbamazepine; D-glucosamine HCl; Polymorphism.

Abbreviations: GLU, glucosamine hydrochloride; DSC, differential scanning calorimetry; XRPD, x-ray powder diffraction; BCS, biopharmaceutical classification system; CBZ, carbamazepine;

SEM, scanning electron microscopy; RH, relative humidity; PSD, particle size distribution; PM, physical mixture.

1. Introduction

The poor aqueous solubility of BCS Class II drugs and new chemical entities is a major problem being faced in pharmaceutical development. The solubility and dissolution rate of these drugs are important determinants of the rate and extent of their absorption from the gastrointestinal tract. In addition, for this class of drugs, dissolution rates are the rate limiting step for bioavailability, therefore enhancing the dissolution rate is crucial to achieving therapeutic blood concentrations. Several techniques have been explored to enhance the dissolution rate of poorly soluble drugs and they include particle size reduction [1], solid dispersion formation [2], complexation [3] and salt formation [4]. The particle size reduction method has been extensively used in attempts to improve dissolution rate of poorly soluble drugs [5, 6] because the reduction in particle size and the subsequent increase in surface area can enhance the dissolution rate and consequently the bioavailability of these pharmaceutical materials. This method is promising but still has some difficulties in its application.

Size reduction of pharmaceutical materials is often performed by a dry milling process, requiring a high energy input, and it has been reported that the strong mechanical forces required (such as grinding) may increase the surface free energy and cause distortion of the crystal lattice as well as reduce particle size [7]. In addition, grinding of hydrophobic drugs usually causes aggregation of drug particles, therefore size reduction by dry milling is limited to around 3 μm due to aggregation between particles at sub-micron diameters [8]. These aggregates have a reduced effective surface area available for dissolution. Size reduction in the nanometer range must be carried out by other techniques such as salt-assisted milling [9]. Recent research has explored particle size reduction to

the submicron range by co-grinding with additives [10 - 13]. Co-grinding is economically and environmentally desirable as, unlike other techniques, it does not require toxic solvents [14] and sophisticated equipment [15].

Pharmaceutical powders usually have insulating properties with relatively small particle size and low bulk density and as such they are susceptible to triboelectric charging, especially during mechanical processing when particles collide with walls of containers and with each other [16, 17].. In addition, particle charging can cause problems in the manufacture of formulations by affecting powder flow, reducing fill and dose uniformity [18, 19]; for example particle charging may cause adhesion and deposition of particles to walls especially in case of fine particles such as in dry powder inhalers [20, 21]. Triboelectrification has been used to study the impact of the counter ion on flurbiprofen salts as a consideration during the preformulation process [22], reduce the charging of flurbiprofen (a drug with a high propensity for charging) in binary mixtures of cellulose ethers [23], ordered mixing [24] and recently as a way of manipulating the charge of their final product of solid dispersions using single solvents and binary mixtures of solvents [25].

Al-Hamidi *et al*., [2] explored the use of D-glucosamine HCl (GLU) as a potential excipient to improve the dissolution rate of poorly soluble drug by use of the co-grinding approach. They also investigated the effect of the order of grinding on dissolution and they found the co-grinding technique to significantly increase the dissolution rate of the poorly soluble drug carbamazepine (CBZ). However, they did not explore the handling issues which may potentially arise as a result of grinding. Given that the grinding process gives rise to charging and that particle triboelectrification plays an important role in powder processing,subsequently affecting the quality of formulations [16], the objectives of this study were to characterise the full charging profiles of pure CBZ and GLU and their co-ground mixtures. As Al-Hamidi *et al* [2] reported GLU as a new carrier for improved dissolution behaviour for poorly soluble drugs, it is important to evaluate its effects on

API handling. To the best of our knowledge, there is no work that has looked at the effects of duration of grinding on co-ground mixtures of the drug and carrier.

2. Materials and Methods

2.1. Materials

Carbamezepine (CBZ) and D-(+)-glucosamine hydrochloride (GLU) were purchased from Sigma-Aldrich (UK). These materials were used as obtained from the supplier.

2.2. Preparation of physical mixtures of drug-carrier

Physical mixtures of CBZ: GLU (5 g in total) were prepared by mixing CBZ and GLU in a Turbula^{TM} blender (Turbula, Basel, Switzerland) for 10 min. Different weight ratios of drug: carrier (1:1, 1:2 and 1:4 w/w) were prepared for comparison purposes. After mixing, the powders were stored in a screw-cap glass vial for one week at room temperature before use.

2.3. Preparation of co-ground mixtures of drug-carrier

Co-grinding of the formulations was conducted according to Al-Hamidi *et al*., [26, 27]. Briefly, co-grinding of different ratios of drug to carrier (1:1, 1:2 and 1:4 w/w) was achieved using a ball mill (Pulverisette 6, Fritsch, Germany). The total amount of drug: carrier was kept constant for all formulations (20 g) during co-grinding process. The volume of the mill chamber was 250 mL. Eight stainless steel balls, with diameter 20 mm, were used and occupied one third of the volume of the chamber. The vibration rate was 400 rpm. The samples (drug: carrier) were subjected to different grinding times (10, 30 and 60 min).

2.4. Scanning electron microscopy (SEM)

Electron micrographs of different samples were obtained using a scanning electron microscope (Leica Cambridge S360, UK) operating at 15 kV. The samples were mounted on a metal stub with double-sided adhesive tape and coated under vacuum with gold in an argon atmosphere prior to observation. Micrographs with different magnifications were recorded to study the morphology of the different samples.

2.5. Particle Size Analysis (PSD)

Particle size distribution plots of all formulations were conducted using a Sympatec laser diffraction particle size analyser (Clausthal-Zellerfeld, Germany). The average particle diameters (D10%, D50%, and D90%) were calculated automatically using the software provided. Approximately 2-3 g of the sample was transferred into the funnel of the VIBRI (vibrator feeder). The sample container was cautiously tapped against the funnel to ensure all of the content was transferred. This was to ensure that the material flowed through the vibrating chute into the groove of the rotary table. All sample data was analysed using the software provided.

2.6. Differential scanning calorimetry (DSC)

Samples of CBZ, GLU and the co-ground formulations (3-6 mg) were placed in standard aluminium pans (40 μL) with a vented lid. The crimped aluminium pans were heated from 20 to 250 ˚C at a scanning rate of 10 °C/min using nitrogen as a purge gas in a DSC 1 (Mettler-Toledo, Switzerland). The enthalpy, onset temperatures and melting points of the samples were obtained using the software provided.

2.7. X-ray powder diffraction (XRPD)

The pure CBZ, GLU and their co-ground samples were characterised by X-ray powder diffraction (XRPD) according to the methodology reported by Laity *et al*., [28] using a D2 Phaser diffractometer (Bruker AXS GmbH, Karlsruhe, Germany), with a sealed microfocus generator operated at 30 kV and 10 mA, producing Cu_{Ka} ($\lambda_X = 0.1542$ nm) radiation and a Lynxeye 'silicon strip' multi-angle detector. The samples were scanned in Bragg-Brantano geometry, over a scattering (Bragg, 2θ) angle range from 5 to 100°, in 0.02° steps at 1.5° min^{-1}.

2.8. Fourier transform infrared (FT-IR)

The pure CBZ, GLU and their co-ground samples were characterised also using FT-IR according to the methodology detailed by Asare-Addo et al. [25]. In brief, a 5–10 mg sample of pure CBZ, pure GLU, Physical mix of CBZ and GLU, CBZ and GLU ground for either 10 min or 60 min (all at a 1:1 ratio) were placed on an attenuated total reflection (ATR) plate and analysed using FTIR spectroscopy (Nicolet 380 FT-IR spectrometer, ThermoElectron Corporation, USA). All samples were analysed by measuring the transmittance of infrared wavelengths of the electromagnetic spectrum of the sample in the range of 400–4000 cm^{-1}.

2.9. Electrostatic properties of physical mixture and solid dispersions

The charge properties of powders were analysed using a recent novel approach developed in our laboratory (Figure 1) and reported in Hussain et al., [17]. The experimental apparatus used to investigate the triboelectrification of powders consists of a single non-contact electrostatic inductive sensor (probe), a charge amplifier unit, a national instrument (NI) data acquisition equipment and personal computer for data recording and processing [17]. The developed method offers distinctive advantages such as the determination of charge level and charge polarity across population of

particles. Electrostatic induction method has been previously used by many researchers to investigate charging properties of particulate materials [29-34].

A similar approach based on induction method to investigate the charge properties of single solid particle or droplets are also reported by other authors [29-31]. The properties of other materials also reported by other authors based on a contact method (particle-electrode) was adapted previously by Masuda and Matsusaka to detect bipolar charge distribution by analysing pulsating electrical signals generated in gas-solid pipe flow due to charge transfer from particle to the metal pipe wall [29-31].

Typical example of processed charge signal obtained as a result of un-grounded GLU particles moving through the sensor using vibratory orifice feeder under gravity is shown in Figure 2. The direction of each peak shows the polarity of charged particles and amplitude from baseline and represents the amount of charge on moving particle. This novel method allows the detection and measurement of charge distribution on the charge sign basis in a population of particles. A sample of each of pure CBZ, GLU and their co-ground mixtures was fed in the cylindrical sensor with the help of the vibratory feeder and conveyed toward the sensor by gravity in a vertical direction. Special care was taken by considering the adhesion properties of the particles with the wall of the sensor. After each experiment, the inner tube was replaced in order to remove any deposits, impurities or surface charge that may have been present on the surface from a previous test. A fresh sample was used for each test experiment. Each sample was analysed six times in a humidity and temperature controlled laboratory maintained at RH= 50 %, 22 ºC). The positive charge is the sum of all positive charges whereas the negative charge is the sum of all negative charges. The net charge is the sum of positive and negative charges. The charge–to–mass ratio (CMR or charge

density) was defined as the charge (negative charge for N–CMR, positive charge for P–CMR, net charge for net–CMR) per unit mass, in nC/g.

3. RESULTS AND DISCUSSION

3.1. Solid state characterization co-ground samples and physical mixtures

Figure 3 shows the initial particle sizes of the sample used prior to the grinding process and Figure 4 shows the SEM images of the starting materials before and after being ground for 10 min. Table 1, shows the particle sizes of the various ratios ground from 10 to 60 min. These results show a dramatic decrease in the average particle diameters (D_{50}%) of pure CBZ after grinding for 10 min, and further significant reduction in particle size was induced by further grinding to 30 and 60 min ($P < 0.05$, ANOVA test). This was also the case for GLU and co-ground mixtures. The aggregation in Figure 4 suggests that the smaller particles which were generated due to the grinding process are inherently more cohesive. It is thought that the surface free energy becomes predominant over the effect of gravitation forces when the particles become very fine. The effect of mechanical stress can result in an increase in the intensity of free electrons at the particle surface thereby increasing the surface free energy of powders dramatically [35]. XRPD showed characteristic diffraction peaks for CBZ form III (β-form) at 2θ of 10.5, 12.95 and 15.2 (Figure 5a) [36, 37]. The XRPD pattern of the pure CBZ and the ground CBZ displayed similar diffraction patterns. This suggests that CBZ particles did not undergo structural modification following grinding for 10 and 60 min (Figure 5a). There was however differences in the relative intensities of their peaks and this were attributed to the differences in the crystal sizes as a result of the grinding process. Figure 5b also showed a significant reduction in the crystallinity of GLU with the grinding time. DSC, however, showed the presence of an extra peak present for the CBZ ground for 60 min (indicated by red arrow, Figure

6a). This suggested that the long grinding time (60 min) induced some degree of polymorphism in the sample (Figure 6a). Pure CBZ displayed a melting peak at 176 ºC, followed by an exothermic peak at 179 ºC (an indication of solid-solid transformation of polymorphic form III to I) and then a sharp endothermic peak at 192 ºC (melting of form I) [38]. These processes were also evident in the ground samples. Grzesiak *et al.* [39] conducted an extensive study into the various polymorphic forms of CBZ. Their experimentation showed that all CBZ forms were transformed to form I (triclinic form) on heating, but this transformation occurred at different temperatures depending on the original polymorph. So at a heating rate of 10 ºC/min, CBZ in its trigonal (form II), P-monoclinic (form III), or C-monoclinic (form IV) exhibited a transformation occuring at 135-170 ºC, 162-175 ºC, or 178-187 ºC respectively, after which they melted at ~190 ºC [39]. The presence of a transition peak at 186 ºC for CBZ ground for 60 min indicates that this sample also contains CBZ form IV as a result of the prolonged grinding time. As a result, it can be concluded that the CBZ subjected to longer grinding times contained mixtures of forms III and IV. Figure 5c shows a reduction in the crystallinity of the samples subjected to the co-grinding process. This was in agreement with work done by Al-Hamidi et al. [26]. Figure 6b, shows glucosamine to have a melting point of 210 °C, which is also in agreement with Asare-Addo et al., [25]. DSC can also be used to reflect miscibility by a shift in the melting endotherm of drug [40-43], as well as identifying different polymorphs [44]. Figure 6c shows the distinctive peak for glucosamine as indicated by the black arrow as well as the melting peak for CBZ in the PM at 1:1 ratio. The samples co-ground for 10 and 60 min showed CBZ peaks similar to those in Figure 6a. The glucosamine peaks were also present but displayed sharper melting endotherms. This means the co-grinding process did not induce any significant changes in the thermal behaviour of CBZ. The absence of any melting point depression indicates that CBZ and GLU are immiscible as the chemical potential of CBZ remained unchanged in the glucosamine [41]. FT-IR data showed characteristic peaks for CBZ in its

unground and ground states (Figure 7). These were found at 3464 cm^{-1} (−NH valence vibration), 1676 cm^{-1} (–CO–R vibration), 1605 and 1593 cm^{-1} (range of –C═C– and –C═O vibrations and –NH deformation). The FT-IR spectra were synonymous with polymorph III [37] and indicated that the grinding was not associated with changes at the molecular level [26].

3.2 Triboelectrification studies

Al-Hamidi et al. reported a remarkable improvement in the dissolution of CBZ using GLU as a hydrophilic carrier using a co-grinding technique [26]. Despite the improvement in the dissolution process, it is known that particle charging can arise due to the grinding process and can cause problems in the manufacture of formulations by affecting powder flow, reducing fill and dose uniformity [18, 19]. This can also cause adhesion and deposition of particles to walls especially in case where the samples have been ground to fine particles [20, 21]. It is therefore important to evaluate the charges associated with the grinding process to allow the assessment of formulations that are easy to handle during manufacturing as well as improving dissolution. Powders may develop different polarities and the magnitude of these charges depends on the intrinsic properties of the powders and the types of surfaces the powders have been in contact with during processing. In general, fine particulates tend to charge negatively, whereas large particles tend to charge positively. Lacks and Levandovsky, 2007 [45] provided a hypothetical mechanism for particle size dependent charging. Assuming that the surface density of trapped electrons is initially the same on all particles, it has been argued that collisions allow electrons trapped in high-energy states on one particle to transfer to the vacant low-energy states on another particle. This has been recently discussed in a recent review [46]. The charge density of the pure CBZ drug was higher than that of pure GLU carrier (1.7 ± 0.4 *versus* 0.5 ± 0.2 nC/g) (Figure 8). This agrees with previous studies, which showed APIs to exhibit generally higher charge densities in comparison to excipients [16].

Charge distribution analyses showed pure CBZ to have a primarily a positive charge behaviour (Figure 9a) whereas pure GLU demonstrated a bipolar charge behaviour (P-CMR and N-CMR of 1.2 ± 0.5 and -0.7 ± 0.3 nC/g respectively) (Figure 9b). After grinding, both ground CBZ (Figure 9a) and ground GLU (Figure 9a) showed primarily positive charge behaviours. The net-charge density of CBZ and GLU generally increased with increasing grinding time, except for CBZ ground for 60 min, which showed a similar charge density to CBZ ground for 10 min (Figure 8).

Regardless of CBZ:GLU ratio, and in contrast to CBZ:GLU physical mixtures that showed bipolar charge behaviours and overall positive net-charge densities (Figures 9c,d,e), all ground CBZ:GLU co-ground mixtures (1:1, 1:2 and 1:4) exhibited primarily electronegative charge behaviours with the highest net-charge density observed for CBZ:GLU ground for 10 min (Figures 9c,d,e). It can be assumed that during the grinding process, electrons are being transferred from the stainless steel surface to the negatively charged powder particles. The effect of both CBZ:GLU ratio and grinding time on the charging properties of ground CBZ:GLU mixtures are shown in Figures 10a and b. It can be observed that the net charge density for ground CBZ:GLU mixtures increased (and the absolute charge density decreased) with increasing duration of grinding (Figures 10a and b). In general, particle charging increases with an increase in the level of energy introduced to the solid particles [20]. The net charge density decreased with increasing CBZ content in CBZ:GLU mixtures up to 30 %, above which the net charge density increased (Figures 10a and b).

4. CONCLUSIONS

Solid states analysis showed polymorphic transformations to occur with the CBZ as a result of the grinding process. Solid-state analysis also showed CBZ and GLU to be crystalline despite increased grinding time. The charge density of the pure CBZ drug was higher than that of pure GLU carrier and showed glucosamine to have a very low charge. As various strategies including co-grinding are

used in the improvement of the solubility of drugs with poor aqueous solubility, it is important to characterize and predict the electrostatic behaviour of such mixtures before and after processing. The results showed the net charge density of the samples to decrease with increasing CBZ content in CBZ:GLU mixtures up to 30 %, above which the net charge density increases. The novel technique reported here for determining the charge of the dispersions could therefore also be used as tool to help a formulator determine the appropriate formulations that enhance dissolution but also improve handling.

5. ACKNOWLEDGEMENTS

The authors would like to acknowledge the University of Huddersfield for financial support.

6. CONFLICT OF INTEREST

All authors declare no conflict of interest

6. REFERENCES

[1] X. Han, C. Ghoroi, D. To, Y. Chen, and R. Davй, Simultaneous micronization and surface modification for improvement of flow and dissolution of drug particles, Int J Pharm. 415 (2011) 185-195.

[2] H. Al-Hamidi, A. A. Edwards, M. A. Mohammad, and A. Nokhodchi, To enhance dissolution rate of poorly water-soluble drugs: Glucosamine hydrochloride as a potential carrier in solid dispersion formulations, Colloids Surf. B. 76 (2010) 170-178.

[3] T. Loftsson and D. Duchкne, Cyclodextrins and their pharmaceutical applications, Int J Pharm. 329 (2007) 1-11.

[4] S. E. David, P. Timmins, and B. R. Conway. Impact of the counterion on the solubility and physicochemical properties of salts of carboxylic acid drugs, Drug Dev Ind. Pharm. 38 (2012) 93-103.

[5] G. Buckton and A. E. Beezer, The relationship between particle size and solubility, Int J Pharm. 82 (1992) R7-R10

[6] A. Martini, C. Torricelli, and R. De Ponti, Physico-pharmaceutical characteristics of steroid/crosslinked polyvinylpyrrolidone coground systems, Int J Pharm. 75 (1991) 141-146.

[7] G. Yamaguchi and K. Sakamoto, Effect of Dry Grinding on Gibbsite, Bull. Chem. Soc. Jpn, 32 (1959) 1364-1368

[8] S. Fadda, A. Cincotti, A. Concas, M. Pisu, and G. Cao, Modelling breakage and re-agglomeration during fine dry grinding in ball milling devices, Powder Technol, 194 (2009) 207-216

[9] V. Mochalin, A. Sagar, S. Gour, and Y. Gogotsi, Manufacturing Nanosized Fenofibrate by Salt Assisted Milling, Pharm Res. 26 (2009) 1365-1370.

[10] M. Kubo, Y. Oumi, R. Miura, A. Stirling, A. Miyamoto, M. Kawasaki, et al., Atomic control of layer-by-layer epitaxial growth on $SrTiO_3$: Molecular-dynamics simulations, Phys. Rev. B, 56 (1997) 13535-13542.

[11] G. G. Liversidge and K. C. Cundy, Particle size reduction for improvement of oral bioavailability of hydrophobic drugs: I. Absolute oral bioavailability of nanocrystalline danazol in beagle dogs, Int. J Pharm. 125 (1995) 91-97.

[12] M. Sugimoto, T. Okagaki, S. Narisawa, Y. Koida, and K. Nakajima, Improvement of dissolution characteristics and bioavailability of poorly water-soluble drugs by novel co-grinding method using water-soluble polymer, Int. J Pharm. 160 (1998) 11-19.

[13] H. Yamada, S. Takahashi, H. Fujita, N. Kobayashi, and S. Okabe, Cytokine-induced neutrophil chemo-attractants in healing of gastric ulcers in rats: expression of >40-kDa chemoattractant in delayed ulcer healing by indomethacin, Dig. Dis. Sci. 44 (1999) 889-95.

[14] M. Sarkari, J. Brown, X. Chen, S. Swinnea, R. O. Williams Iii, and K. P. Johnston, Enhanced drug dissolution using evaporative precipitation into aqueous solution, Int. J Pharm. 243 (2002) 17-31.

[15] M. Moneghini, I. Kikic, D. Voinovich, B. Perissutti, and J. Filipovic-Grcic, Processing of carbamazepine-PEG 4000 solid dispersions with supercritical carbon dioxide: preparation, characterisation, and in vitro dissolution, Int. J Pharm. 222 (2001) 129-38.

[16] E. Supuk, A. Zarrebini, J. P. Reddy, H. Hughes, M. M. Leane, M. J. Tobyn, et al., Tribo-electrification of active pharmaceutical ingredients and excipients, Powder Technol. 217 (2012) 427-434.

[17] T. Hussain, W. Kaialy, T. Deng, M. S. A. Bradley, A. Nokhodchi, and D. Armour-Chйlu, A novel sensing technique for measurement of magnitude and polarity of electrostatic charge distribution across individual particles, Int. J Pharm. 441 (2013) 781-789.

[18] J. N. Stainforth, "The importance of electrostatic measurements in aerosol formulation and reformulation, Respir. Drug Deliv. IV (1994) 303-311.

[19] H. Watanabe, M. Ghadiri, T. Matsuyama, Y. L. Ding, K. G. Pitt, H. Maruyama, et al., Triboelectrification of pharmaceutical powders by particle impact, Int. J Pharm. 334 (2007) 149-155.

[20] A. G. Bailey, A. H. Hashish, and T. J. Williams, Drug delivery by inhalation of charged particles, J Electrostat. 44 (1998) 3-10.

[21] S. Karner and N. Anne Urbanetz, The impact of electrostatic charge in pharmaceutical powders with specific focus on inhalation-powders, J Aerosol Sci., 42 (2011) 428-445.

[22] E. Supuk, M. U. Ghori, K. Asare-Addo, P. R. Laity, P. M. Panchmatia, and B. R. Conway, The influence of salt formation on electrostatic and compression properties of flurbiprofen salts, Int. J Pharm., 458 (2013) 118-27.

[23] M. U. Ghori, E. Supuk, and B. R. Conway, Tribo-electric charging and adhesion of cellulose ethers and their mixtures with flurbiprofen, Eur. J Pharm Sci., 65 (2014) 1-8.

[24] K. Asare-Addo, W. Kaialy, M. Levina, A. Rajabi-Siahboomi, M. U. Ghori, E. Supuk, et al., The influence of agitation sequence and ionic strength on in vitro drug release from hypromellose (E4M and K4M) ER matrices-the use of the USP III apparatus, Colloids Surf. B., 104, (2013) 54-60.

[25] K. Asare-Addo, E. Supuk, H. Al-Hamidi, S. Owusu-Ware, A. Nokhodchi, and B. R. Conway, Triboelectrification and dissolution property enhancements of solid dispersions, Int. J Pharm., 485 (2015) 306-16.

[26] H. Al-Hamidi, A. A. Edwards, M. A. Mohammad, and A. Nokhodchi, Glucosamine HCl as a new carrier for improved dissolution behaviour: effect of grinding, Colloids Surf. B., 81 (2010) 96-109.

[27] H. Al-Hamidi, A. A. Edwards, D. Douroumis, K. Asare-Addo, A. M. Nayebi, S. Reyhani-Rad, et al., Effect of glucosamine HCl on dissolution and solid state behaviours of piroxicam upon milling, Colloids Surf. B., 103 (2013) 189-99.

[28] P. R. Laity, K. Asare-Addo, F. Sweeney, E. Šupuk, and B.R. Conway, Using small-angle X-ray scattering to investigate the compaction behaviour of a granulated clay, Appl. Clay Sci., 108 (2015) 149-164.

[29] H. Watanabe, T. Matsuyama and H. Yamamoto, Experimental study on electrostatic atomization of highly viscous liquids, J Electrostat. 57 (2003) 183-197.

[30] T. Matsumaya and H. Yamamoto, Characterizing the electrostatic charging of polymer particles by impact charging experiments, Adv. Powder Technol., 6 (1995) 211-220.

[31] P.H.W. Vercoulen, Electrostatic processing of particles, A tool in particle technology, CHEM 23 (1995).

[32] M. Murtomaa, E. Rasanen, J. Rantanen, A. Bailey, E. Laine, J. Mannermaa and J. Yliruusi, Electrostatic measurements on a miniaturized fluidized bed, J Electrostat., 57 (2003) 91-106.

[33] D. I. Armour-Chelu and S. R. Woodhead, Comparison of the electric charging properties of particulate materials in gas–solids flows in pipelines, J Electrostat, 56 (2002) 87-101.

[34] J. B. Gajewski, Non-contact electrostatic flow probes for measuring the flow rate and charge in the two-phase gas–solids flows, Chem. Eng. Sci., 61 (2006) 2262-2270.

[35] J. C. Feeley, P. York, B. S. Sumby, and H. Dicks, Comparison of the surface properties of salbutamol sulphate prepared by micronization and a supercritical fluid technique, J Pharm Pharmacol, 50 (1998) 54-54.

[36] A. Nokhodchi, N. Bolourtchian, and R. Dinarvand, Dissolution and mechanical behaviors of recrystallized carbamazepine from alcohol solution in the presence of additives, J Cryst. Growth, 274 (2005) 573-584.

[37] C. Rustichelli, G. Gamberini, V. Ferioli, M. C. Gamberini, R. Ficarra, and S. Tommasini, Solid-state study of polymorphic drugs: carbamazepine, J Pharmaceut. Biomed., 23 (2000) 41-54.

[38] A. Nokhodchi, H. Al-Hamidi, M.D. Antonijevic, S. Owusu-Ware and W. Kaialy Dissolution and solid state behaviours of carbamazepine-gluconolactone solid dispersion powders: The potential use of gluconolactone as dissolution enhancer. Chem. Eng. Res. Des. (2015) (In press)

[39] A. L. Grzesiak, M. Lang, K. Kim, and A. J. Matzger, Comparison of the four anhydrous polymorphs of carbamazepine and the crystal structure of form I, J Pharm Sci., 92 (2003) 2260-71.

[40] J.L. Ford, P. Timmins, Pharmaceutical Thermal Analysis. Ellis Horwood, New York (1987).

[41] J. Gupta, C. Nunes, S. Vyas and S. Jonnalagadda, Prediction of solubility parameters and miscibility of pharmaceutical compounds by molecular dynamics simulations. J Phys Chem. B, 115 (2011), 2014–2023.

[42] P. Mura, M.T. Faucci, A. Manderioli, S. Furlanetto, S. Pinzauti, Thermal analysis as a screening technique in preformulation studies of picotamide solid dosage forms. Drug Dev Ind Pharm, 24 (1998), 747–756.

[43] S.L. Shamblin, L.S. Taylor and G. Zografi, Mixing behaviour of colyophilized binary systems, J Pharm Sci, 87 (1998) 694 - 701.

[44] K.J. Crowley and G. Zografi, Cryogenic grinding of indomethacin polymorphs and solvates: assessment of amorphous phase formation and amorphous phase physical stability, J Pharm Sci., 91 (2002) 492-507.

[45] D. J. Lacks and A. Levandovsky, Effect of particle size distribution on the polarity of triboelectric charging in granular insulator systems, J Electrostat, 65 (2007) 107–112.

[46] W. Kaialy, A review of factors affecting electrostatic charging of pharmaceuticals and adhesive mixtures for inhalation, Int J Pharm. (2016) In press. doi: 10.1016/j.ijpharm.2016.01.076

Tables

Table 1. Particle size analysis of pure carbamazepine, glucosamine and their co-ground mixtures

Formulation	Grinding time (min)	$D_{10\%}$ (μm)	$D_{50\%}$ (μm)	$D_{90\%}$ (μm)
CBZ	10	1.52	31.55	272.55
GLU	10	0.85	5.20	120.60
CG 1:1	10	1.75	27.91	239.42
GG 1:2	10	1.57	17.61	143.34
CG 1:4	10	1.41	20.86	280.02
CBZ	30	1.48	24.48	276.55
GLU	30	1.15	13.30	132.90
CG 1:1	30	2.13	31.35	236.85
GG 1:2	30	2.20	27.85	192.38
CG 1:4	30	1.56	28.51	279.18
CBZ	60	1.37	15.87	261.61
GLU	60	1.11	9.80	113.04
CG 1:1	60	2.21	28.42	203.15
GG 1:2	60	1.80	22.82	208.28
CG 1:4	60	2.65	36.10	282.44

Figure Titles

Figure 1. Schematic of experimental setup used in the determination of the formulations charge.

Figure 2. Particle size analysis of a) pure CBZ, GLU and physical mixes of carbamazepine (CBZ) and glucosamine

Figure 3. SEM images a) CBZ b) CBZ 60 min ground c) GLU d) GLU 60 min ground e) PM CBZ-GLU f) ratio 1:1 60 min ground

Figure 4. XRD pattern of a) pure CBZ and CBZ ground for 10 and 60 min, b) pure GLU and GLU ground for 10 and 60 min, c) CBZ:GLU 1:1 physical mix ratio and same ratio ground for 10 and 60 min.

Figure 5. DSC plot of a) pure CBZ and CBZ ground for 10 and 60 min, b) pure GLU and GLU ground for 10 and 60 min, c) CBZ:GLU 1:1 physical mix ratio and same ratio ground for 10 and 60 min.

Figure 6. FT-IR spectrum of a) pure CBZ, b) pure GLU, c) GLU ground for 10, d) GLU ground for 60 min, e) CBZ:GLU 1:1 physical mix, f) CBZ:GLU 1:1 co-ground for 10 min, g) CBZ:GLU 1:1 co-ground for 60 min, h) CBZ ground for 10 and i) CBZ ground for 60 min.

Figure 7. Net- charge to mass ratio (net-CMR) for pure carbamazepine (CBZ), pure glucosamine HCl (GLU) and physical mixtures of CBZ:GLU at different ratios (1:1, 1:2 and 1:4, w:w) ground for different times (10, 30 and 60 min).

Figure 8. Positive-charge to mass ratio (P-CMR) and negative-charge to mass ratio (N-CMR) for pure carbamazepine (CBZ) (**a**), pure glucosamine HCl (GLU) (**b**) and physical mixtures of CBZ:GLU at 1:1 (**c**), 1:2 (**d**) and 1:4 (**e**) ratios (w:w) ground for different times (10, 30 and 60 min).

Figure 9. Surface plot (**a**) and contour plot (**b**) of net-CMR in relation to % CBZ in CBZ:GLU mixture and grinding times (min).

Figures

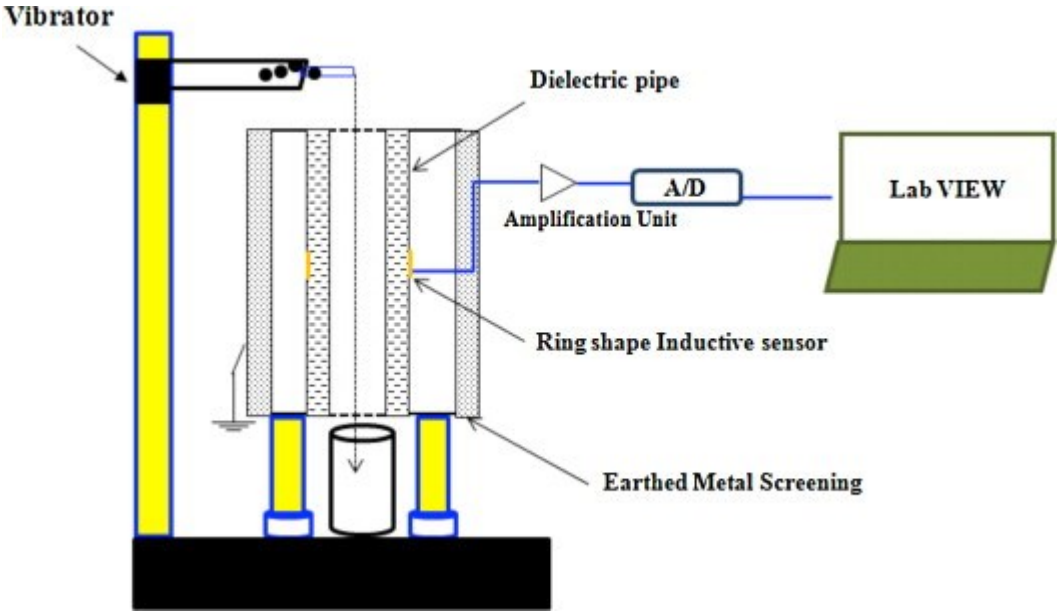

Figure 1.

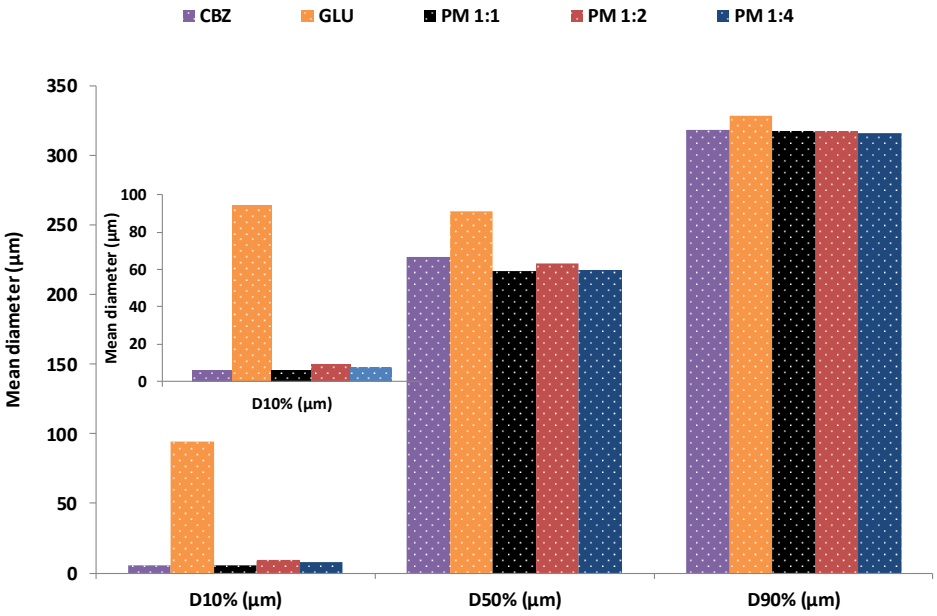
CBZ
GLU
PM 1:1
PM 1:2
PM 1:4
Mean diameter (µm)
350
300
250
200
150
100
50
0
D10% (µm)
D50% (µm)
D90% (µm)
Mean diameter (µm)
100
80
60
40
20
0
D10% (µm)

Figure 2.

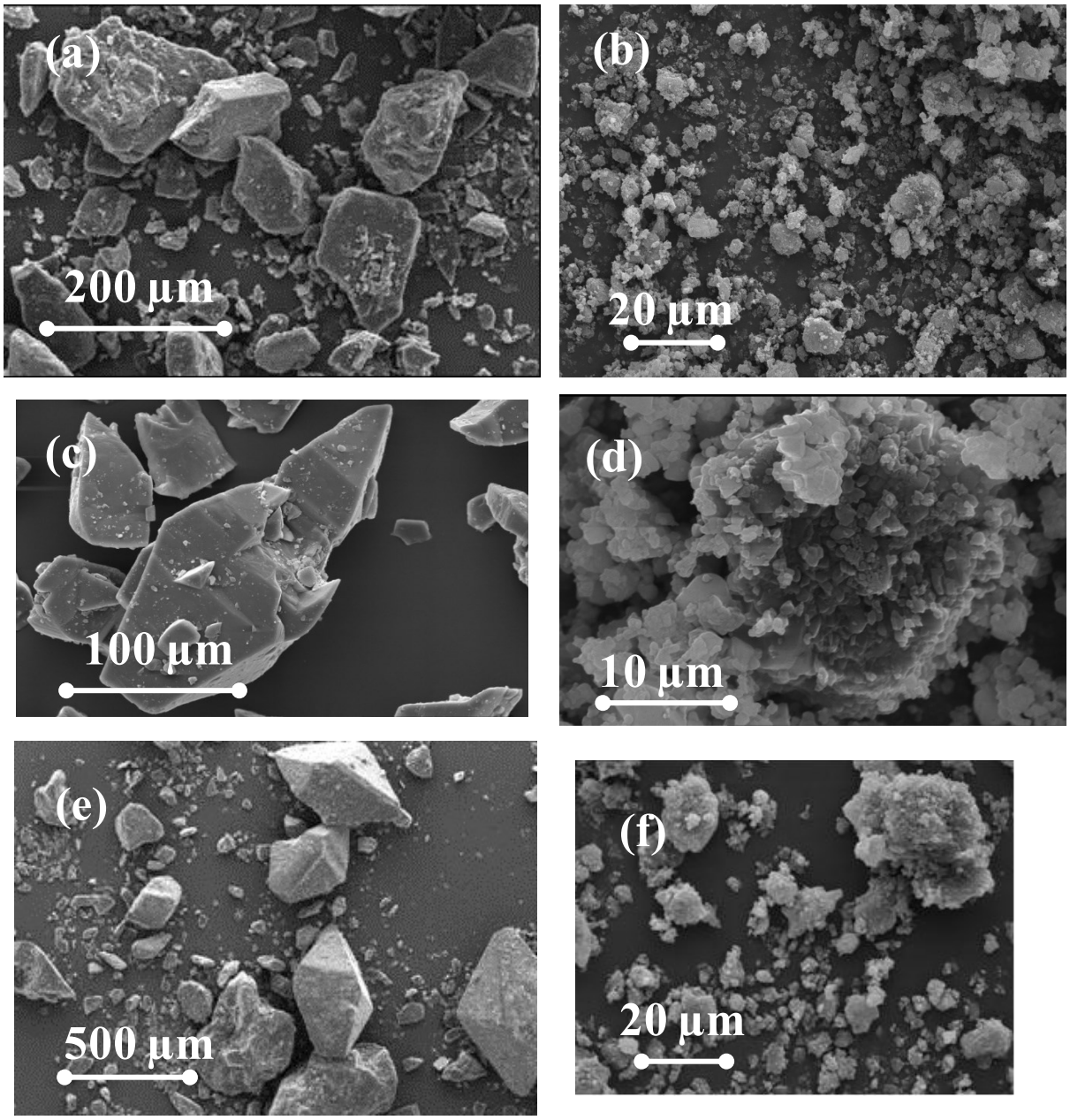

Figure 3.

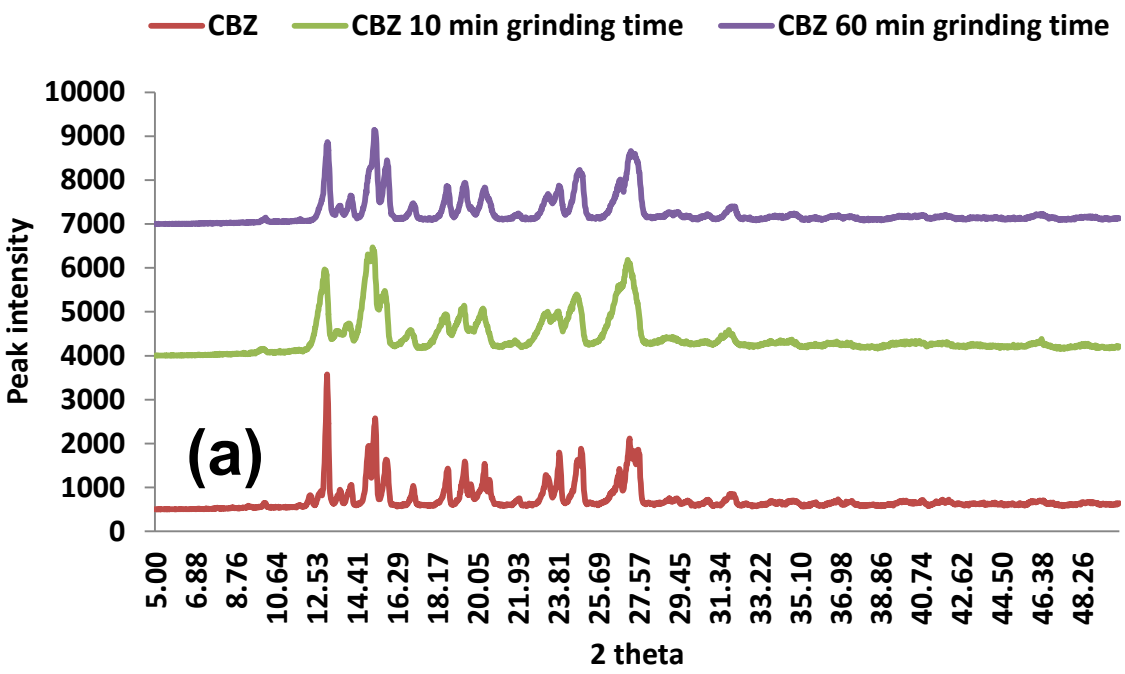
CBZ
CBZ 10 min grinding time
CBZ 60 min grinding time
Peak intensity
10000
9000
8000
7000
6000
5000
4000
3000
2000
1000
0
(a)
5.00
6.88
8.76
10.64
12.53
14.41
16.29
18.17
20.05
21.93
23.81
25.69
27.57
29.45
31.34
33.22
35.10
36.98
38.86
40.74
42.62
44.50
46.38
48.26
2 theta

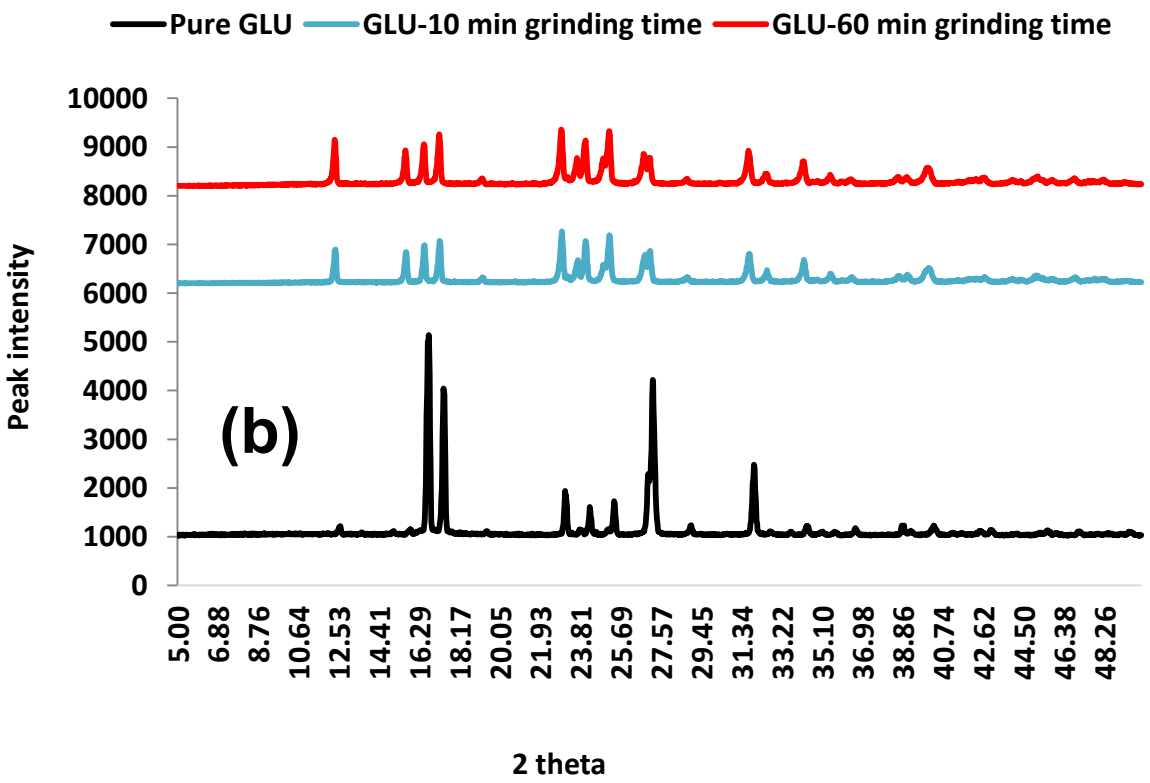
Pure GLU
GLU-10 min grinding time
GLU-60 min grinding time
Peak intensity
10000
9000
8000
7000
6000
5000
4000
3000
2000
1000
0
(b)
5.00
6.88
8.76
10.64
12.53
14.41
16.29
18.17
20.05
21.93
23.81
25.69
27.57
29.45
31.34
33.22
35.10
36.98
38.86
40.74
42.62
44.50
46.38
48.26
2 theta

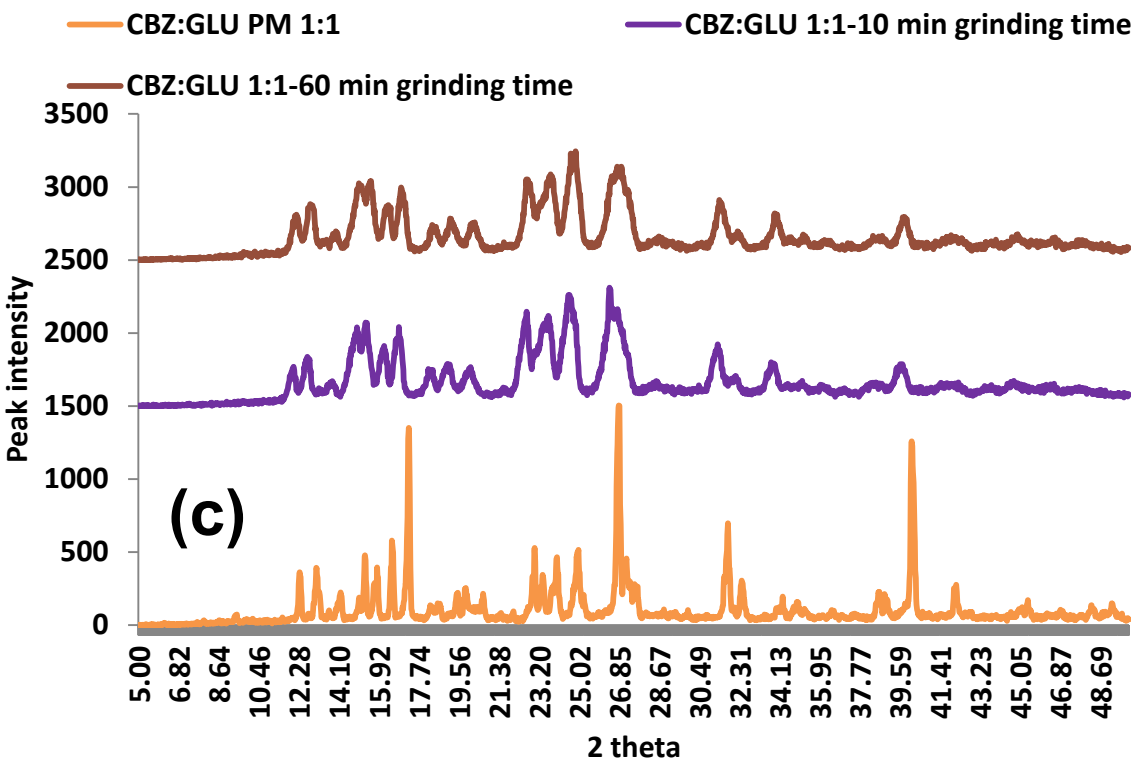
CBZ:GLU PM 1:1
CBZ:GLU 1:1-10 min grinding time
CBZ:GLU 1:1-60 min grinding time
Peak intensity
3500
3000
2500
2000
1500
1000
500
0
(c)
5.00
6.82
8.64
10.46
12.28
14.10
15.92
17.74
19.56
21.38
23.20
25.02
26.85
28.67
30.49
32.31
34.13
35.95
37.77
39.59
41.41
43.23
45.05
46.87
48.69
2 theta

Figure 4.

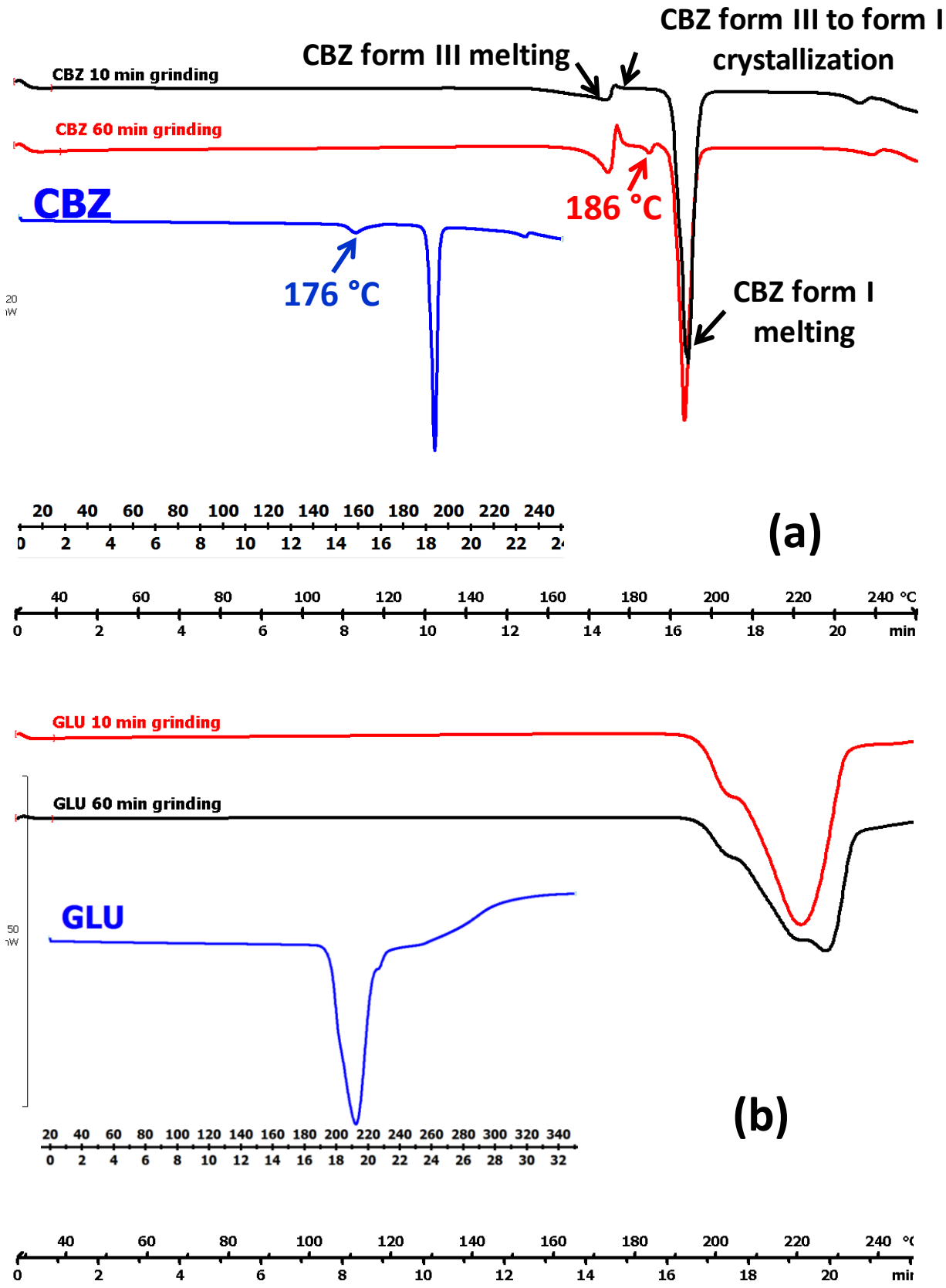
CBZ form III to form I crystallization
CBZ form III melting
CBZ 10 min grinding
CBZ 60 min grinding
CBZ
186 °C
176 °C
CBZ form I melting
20 40 60 80 100 120 140 160 180 200 220 240
0 2 4 6 8 10 12 14 16 18 20 22
(a)
40 60 80 100 120 140 160 180 200 220 240 °C
0 2 4 6 8 10 12 14 16 18 20 min
GLU 10 min grinding
GLU 60 min grinding
GLU
20 40 60 80 100 120 140 160 180 200 220 240 260 280 300 320 340
0 2 4 6 8 10 12 14 16 18 20 22 24 26 28 30 32
(b)
40 60 80 100 120 140 160 180 200 220 240
0 2 4 6 8 10 12 14 16 18 20

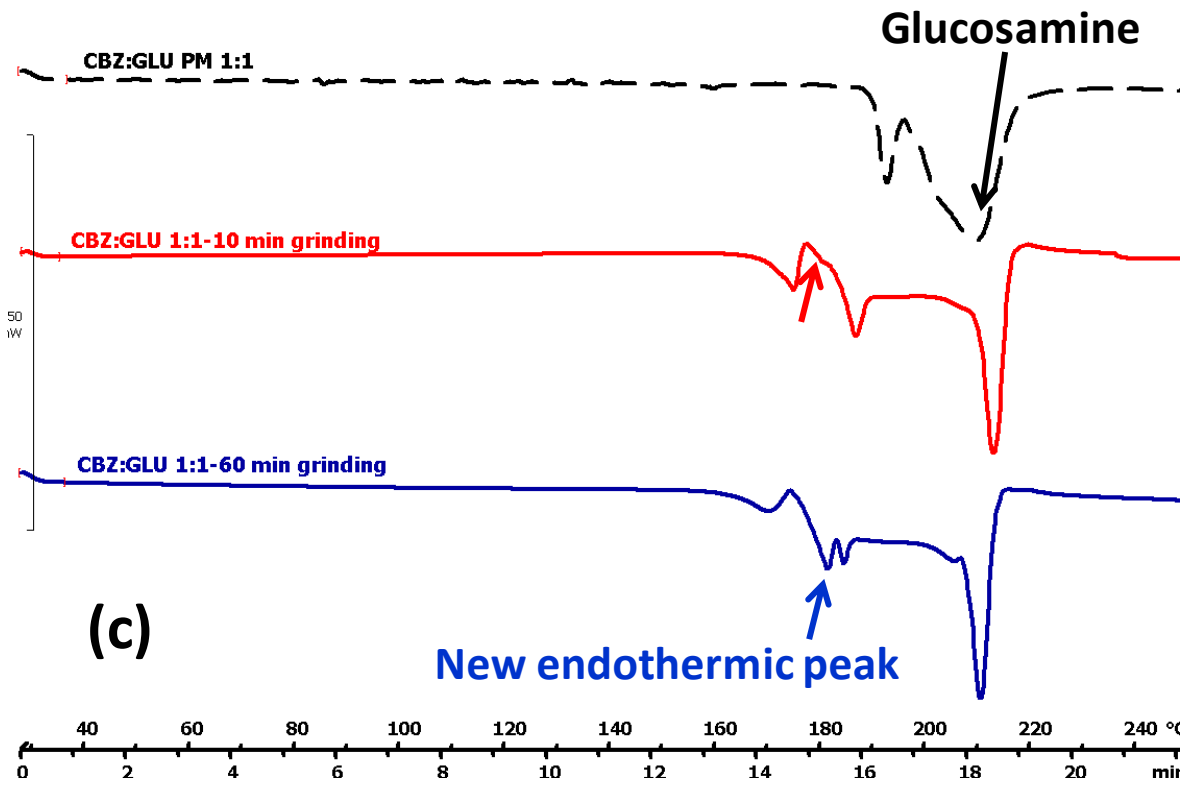
Glucosamine
CBZ:GLU PM 1:1
CBZ:GLU 1:1-10 min grinding
50
W
CBZ:GLU 1:1-60 min grinding
(c)
New endothermic peak
40
60
80
100
120
140
160
180
200
220
240 °C
0
2
4
6
8
10
12
14
16
18
20
min

Figure 5.

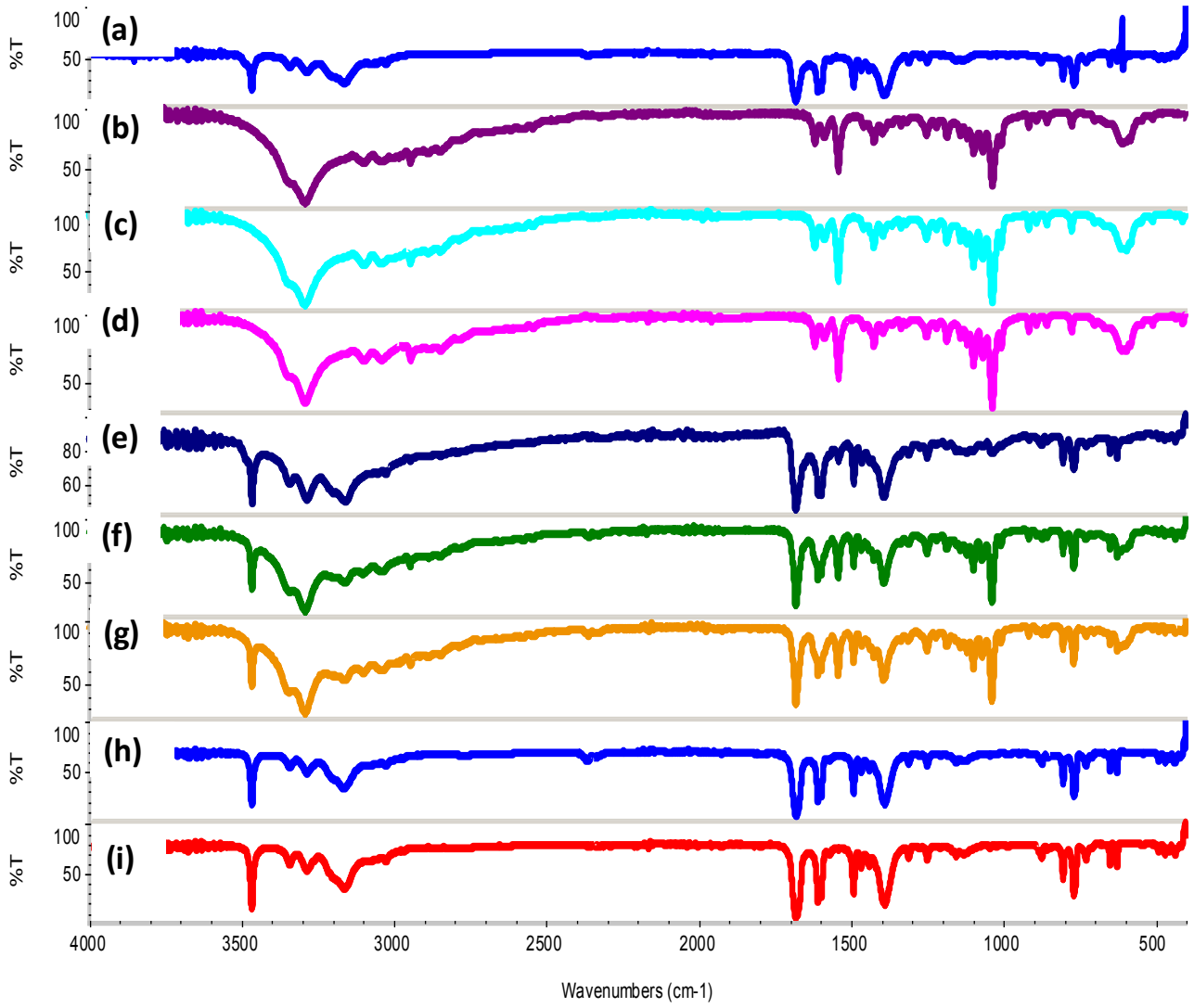
(a)
(b)
(c)
(d)
(e)
(f)
(g)
(h)
(i)
%T
100
50
80
60
4000
3500
3000
2500
2000
1500
1000
500
Wavenumbers (cm-1)

Figure 6.

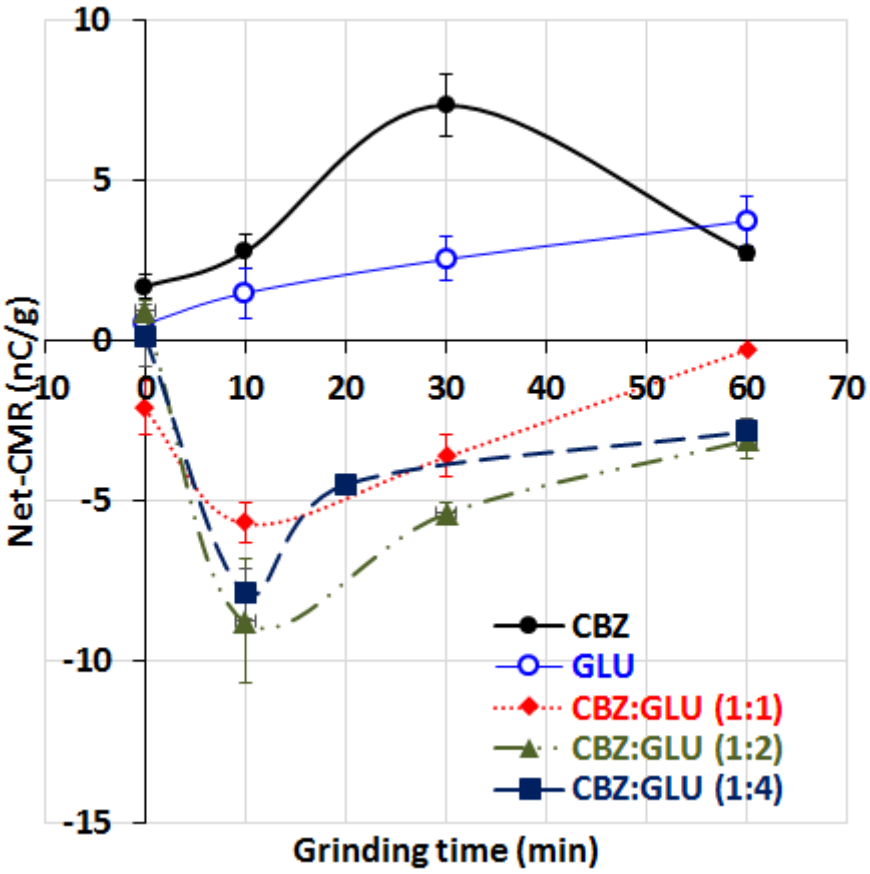
10
5
0
-5
-10
-15
-10
0
10
20
30
40
50
60
70
Net-CMR (nC/g)
Grinding time (min)
CBZ
GLU
CBZ:GLU (1:1)
CBZ:GLU (1:2)
CBZ:GLU (1:4)

Figure 7.

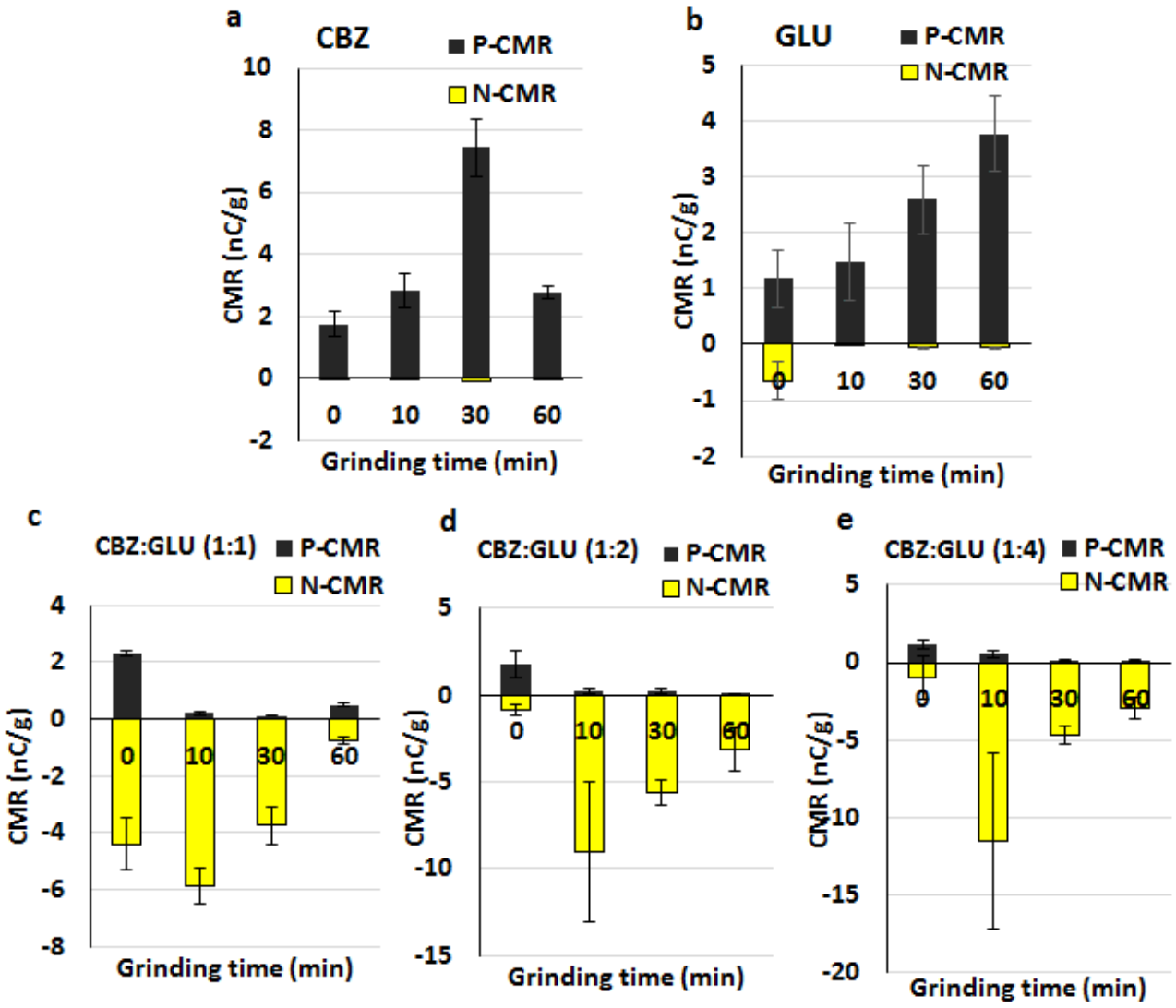
a
CBZ
P-CMR
N-CMR
CMR (nC/g)
Grinding time (min)
b
GLU
P-CMR
N-CMR
CMR (nC/g)
Grinding time (min)
c
CBZ:GLU (1:1)
P-CMR
N-CMR
CMR (nC/g)
Grinding time (min)
d
CBZ:GLU (1:2)
P-CMR
N-CMR
CMR (nC/g)
Grinding time (min)
e
CBZ:GLU (1:4)
P-CMR
N-CMR
CMR (nC/g)
Grinding time (min)

Figure 8.

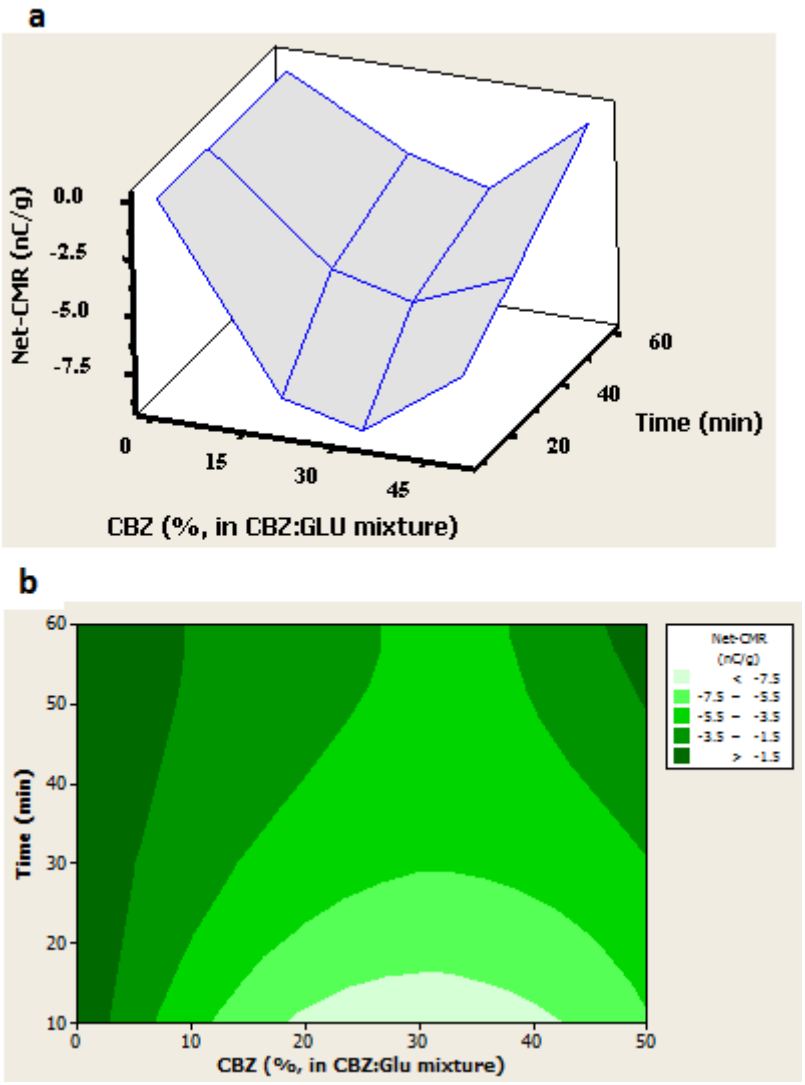
a
Net-CMR (nC/g)
0.0
-2.5
-5.0
-7.5
0
15
30
45
CBZ (%, in CBZ:GLU mixture)
20
40
60
Time (min)
b
Time (min)
60
50
40
30
20
10
0
10
20
30
40
50
CBZ (%, in CBZ:Glu mixture)
Net-CMR
(nC/g)
< -7.5
-7.5 – -5.5
-5.5 – -3.5
-3.5 – -1.5
> -1.5

Figure 9.